2025 8th International Conference on Energy, Electrical and Power Engineering (CEEPE) | 979-8-3315-2184-4/25/$31.00 ©2025 IEEE | DOI: 10.1109/CEEPE64987.2025.11034277

Distributed Energy Storage System Siting and Sizing Method Considering Photovoltaic Hosting Capacity Enhancement

Kai Yuan*
State Grid Economic and Technological Research Institute Co. Ltd
Beijing, China
yuankai83@126.com

Zhiwei Wan
State Grid Economic and Technological Research Institute Co. Ltd
Beijing, China
376347704@qq.com

Chongbo Sun
State Grid Economic and Technological Research Institute Co. Ltd
Beijing, China
sunchongbo2016@163.com

Yudi Ding
State Grid Economic and Technological Research Institute Co. Ltd
Beijing, China
411470317@qq.com

Ming Nie
State Grid Economic and Technological Research Institute Co. Ltd
Beijing, China
582494889@qq.com

Xiao Liu
State Grid Economic and Technological Research Institute Co. Ltd
Beijing, China
liuxiao041@126.com

***Abstract*—The large-scale integration of renewable energy sources has imposed more stringent requirements on the hosting capacity of distribution networks. This paper proposes a distributed energy storage siting and sizing method considering the enhancement in photovoltaic hosting capacity. The method comprehensively considers the operational state of the distribution network and the increased PV hosting capacity following the integration of distributed energy storage. The distributed energy storage planning model is established to determine the optimal DESS planning scheme and enhance the PV hosting capacity of distribution networks. Finally, the effectiveness of the proposed method is verified based on a modified IEEE 33-bus test case. Results show that the proposed method can maximize the PV hosting capacity of distribution networks while ensuring economic benefits and security.**

Keywords—PV hosting capacity, distribution network, distributed energy storage system, siting and sizing

I. INTRODUCTION

With the increasing global demand for clean energy, the photovoltaic (PV) has witnessed a substantial increase in adoption [1]-[2]. However, the intermittent and uncertainty of the large-scale PV integration poses severe challenges to the security operation of distribution networks (DNs), which substantially constrains the PV hosting capacity [3]-[4]. Therefore, the enhancement of PV hosting capacity (PVHC) in DNs is of significant importance for improving renewable energy accommodation levels.

Various methods have been proposed in existing research to enhance the PVHC of DNs. Reference [5] optimized the reactive power control of PV inverters to enhance PVHC and improve voltage quality. The author of [6] proposed an interval estimation method to improve PVHC and quantify overvoltage risks. Reference [7] optimized power flow distribution through DNs reconfiguration, enhancing the PVHC of DNs. However, the above research primarily investigates the hosting capacity enhancement through PV inverters. The potential of distributed energy storage systems (DESSs) for hosting capacity enhancement needs further research.

DESSs are widely used in optimizing the power flow of DNs and mitigating the impact of PV intermittency [8]. Therefore, DESSs exhibit significant potential for enhancing PVHC [9]. An optimal energy storage scheduling method has been formulated in [10] to solve the PVHC enhancement problem. Reference [11] demonstrated through simulation analysis that DESS can effectively improve power flow distribution and enhance PVHC in DNs. However, the above method of using DESS to enhance PVHC does not consider the optimal siting and sizing of DESS. The planning of DESS is of great importance for the safe operation of the DN and for the PVHC enhancement. Therefore, DESS planning methods considering PVHC enhancement in the DN should be further studied.

This paper proposes a DESS siting and sizing method considering PVHC enhancement. Comprehensively considering the operational state of DNs, a DESS planning model is constructed to improve PVHC. Further, the model is solved by second-order cone transformation to derive the DESS planning method. The increase in PV hosting capacity can not only reduce system operating costs, thereby improving economic efficiency, but also increase the maximum allowable PV integration capacity in the future, thereby enabling greener electricity consumption. Finally, the proposed planning method is validated by a modified IEEE 33-bus test case. The optimized

Project supported by Science and Technology Project of State Grid Corporation of China. (5419-202356782A-3-8-KJ).

planning of DESS maximizes the PVHC of the DN while achieving optimal economic benefits in system operation.

II. DESS Planning Model Considering PVHC Enhancement

The optimal siting and sizing of DESS can maximize the enhancement of PVHC. Considering the significant differences in PV and load, the DESS planning model is established in this section to derive the optimal planning method of DESS. The proposed model is shown as follows.

A. Objective Function

The comprehensive objective function for DESS planning incorporates the construction, operation, and maintenance costs of DESS. Besides, the revenue from PVHC enhancement is also considered to quantify the PVHC of DNs. The objective function is formulated as follows:

1) Comprehensive Objective Function f :

$$\min f = f^{IDESS} + f^{ODESS} + f^{loss} + f^{PVHC} \tag{1}$$

where f^{IDESS} represents the annual equivalent installation cost of DESS; f^{ODESS} represents the annual operation and maintenance cost of DESS; f^{loss} represents the annual active power loss cost of the DN; f^{PVHC} represents the revenue cost from PVHC enhancement in the DN.

2) Annual Equivalent Installation Cost of DESS f^{IDESS} :

$$f^{IDESS} = \frac{r(1+r)^{y_{DESS}}}{(1+r)^{y_{DESS}} - 1} \sum_{i \in \Omega_n} \left(C_{IE} S_i^{DESS} + C_{IP} P_i^{DESS} \right) \tag{2}$$

where r represents the discount rate; y^{DESS} represents the service life of DESS; Ω_n represents the set of buses in the DN; C_{IE} and C_{IP} represent the unit capacity investment cost and unit power investment cost of DESS, respectively; S_i^{DESS} and P_i^{DESS} represent the rated capacity and rated power of DESS connected at bus i, respectively.

3) Annual Operation and Maintenance Cost of DESS f^{ODESS} :

$$f^{ODESS} = \sum_{t=1}^{T} \sum_{i \in \Omega_n} C_{ODESS} \left(p_{ch,s,t,i}^{DESS} + p_{dis,s,t,i}^{DESS} \right) \tag{3}$$

where T represents 8760 hours per year; C_{ODESS} represents the operation and maintenance cost per unit of charge/discharge quantity of DESS; $p_{ch,s,t,i}^{DESS}$ and $p_{dis,s,t,i}^{DESS}$ represent the charging power (greater than 0) and discharging power (greater than 0) of the bus accessing the DESS at the time under the scenario, respectively. Note that the charging and discharging power of the DESS here should use the charging and discharging power under typical operation scenarios.

4) Annual Active Power Loss Cost of the DN f^{loss} :

$$f^{loss} = C_{loss} \sum_{t=1}^{T} \sum_{ij \in \Omega_b} r_{ij} I_{s,t,ij}^2 \tag{4}$$

where C_{loss} represents the unit price of the DN losses; Ω_b represents the set of all branches in the DN; r_{ij} represents the resistance of branch ij ; $I_{s,t,ij}$ represents the current magnitude on branch ij at time t under scenario s .

5) PVHC Revenue Cost of the DN f^{PVHC} :

$$f^{PVHC} = -C_{PVHC} \sum_{i \in \Omega_n} P_i^{PVHC} \tag{5}$$

where C_{PVHC} represents the unit revenue cost per increase in PVHC; P_i^{PVHC} represents the increased active power of PV integration at bus i . f^{PVHC} is always negative, meaning that the greater the enhancement in PVHC, the smaller its value becomes.

B. Constraints for Collaborative Planning and Construction of DESS

The following DESS planning constraints need to be considered to ensure the reliable operation of DNs. Based on the typical daily scenarios and PVHC enhancement scenario of the DN, operational constraints for the DN are established. The optimization variables conclude PVHC enhancement level, bus voltages, line power flows, line losses, and DESS charging/discharging power.

1) Inequality Constraints for DESS Planning and Construction

To ensure the safe operation of DESS, the following constraints are considered.

$$0 \le S_i^{DESS} \le S_{\max}^{DESS} \tag{6}$$

$$0 \le P_i^{DESS} \le S_i^{DESS} \tag{7}$$

where $S_{\max}^{DESS}$ represents the maximum rated capacity of DESS allowed to be connected to the DN.

2) Equality Constraints for DESS Planning and Construction

During the planning process, the limitations of the single-unit capacity of the DESS capacitor submodule are considered, and the minimum planning capacity and power of the DESS are set.

$$S_i^{DESS} = n_S^{DESS} m_{S,i}^{DESS} \tag{8}$$

$$P_i^{DESS} = n_P^{DESS} m_{P,i}^{DESS} \tag{9}$$

where n_S^{DESS} and n_P^{DESS} represent the unit rated capacity and rated power of the DESS, respectively; $m_{S,i}^{DESS}$ and $m_{P,i}^{DESS}$

represent non-negative integer variables corresponding to the rated capacity and rated power of the ESS connected at bus i, respectively.

Based on typical daily operation scenarios, economic operation constraints for the DN under typical operating conditions are established, with bus voltages, line power flows, line losses, and DESS charging/discharging power as optimization variables.

3) DESS Operation Constraints

To ensure the normal and long-term operation of DESS after being connected to the DN, the following constraints are imposed on its charging/discharging power and state of charge (SOC).

$$0 \le p_{ch.s.t.i}^{DESS} \le P_i^{DESS} \tag{10}$$

$$0 \le p_{dis,s,t,i}^{DESS} \le P_i^{DESS} \tag{11}$$

$$p_{ch.s.t.i}^{DESS} \le \delta_{ch,s,t,i}^{DESS} M^{DESS} \tag{12}$$

$$p_{dis,s,t,i}^{DESS} \le \delta_{dis,s,t,i}^{DESS} M^{DESS} \tag{13}$$

$$\delta_{ch,s,t,i}^{DESS} + \delta_{dis,s,t,i}^{DESS} \le 1 \tag{14}$$

$$S_i^{DESS} e_{\min}^{SOC} \le E_{s,t,i}^{DESS} \le S_i^{DESS} e_{\max}^{SOC} \tag{15}$$

$$E_{s,t+1,i}^{DESS} = E_{s,t,i}^{DESS} + \eta_{ch}^{DESS} p_{ch,s,t,i}^{DESS} \Delta t - \frac{1}{\eta_{dis}^{DESS}} p_{dis,s,t,i}^{DESS} \Delta t \tag{16}$$

$$\sum_{t=1}^{H} \eta_{ch}^{DESS} p_{ch,s,t,i}^{DESS} \Delta t - \frac{1}{\eta_{dis}^{DESS}} p_{dis,s,t,i}^{DESS} \Delta t = 0 \tag{17}$$

where $\delta_{ch,s,t,i}^{DESS}$ and $\delta_{dis,s,t,i}^{DESS}$ represent the charging state and discharging state, respectively, of the DESS connected at bus i at time t under scenario s. Both are binary variables, and 1 indicates the state is active; M^{DESS} represents a sufficiently large constant; $e_{\min}^{SOC}$ and $e_{\max}^{SOC}$ represent the minimum and maximum allowable SOC of the DESS, respectively; $E_{s,t,i}^{DESS}$ represents the SOC of the DESS connected at bus i at time t under scenario s; η_{ch}^{DESS} and η_{dis}^{DESS} represent the charging efficiency and discharging efficiency of the DESS, respectively; Δt represents the time step, set to 1 hour in this model; H represents one cycle, set to 24 hours in this model. It is worth noting that (25) indicates that the SOC of the DESS at the beginning and end of a cycle should be equal.

4) Power Flow Constraints of the DN

The branch power flow method is used to model the fundamental power flow constraints of the DN considering PVHC enhancement.

$$\sum_{ji \in \Omega_b} \left(P_{s,t,ji} - r_{ij} I_{s,t,ij}^2 \right) + P_{s,t,i} = \sum_{ik \in \Omega_b} P_{s,t,ik} \tag{18}$$

$$\sum_{ji \in \Omega_b} \left(Q_{s,t,ji} - x_{ij} I_{s,t,ij}^2 \right) + Q_{s,t,i} = \sum_{ik \in \Omega_b} Q_{s,t,ik} \tag{19}$$

$$\begin{aligned} & U_{s,t,i}^2 - U_{s,t,j}^2 + \left(r_{ij}^2 + x_{ij}^2 \right) I_{s,t,ij}^2 - \\ & 2\left(r_{ij} P_{s,t,ij} + x_{ij} Q_{s,t,ij} \right) = 0 \end{aligned} \tag{20}$$

$$I_{s,t,ij}^2 U_{s,t,i}^2 = P_{s,t,ij}^2 + Q_{s,t,ij}^2 \tag{21}$$

$$\begin{aligned} P_{s,t,i} = & P_{s,t,i}^{DG} - p_{ch,s,t,i}^{DESS} + p_{dis,s,t,i}^{DESS} \\ & - P_{s,t,i}^{LOAD} - P_{s,t,i}^{EV} + P_i^{PVHC} \end{aligned} \tag{22}$$

$$Q_{s,t,i} = Q_{s,t,i}^{DG} - Q_{s,t,i}^{LOAD} \tag{23}$$

$$P_i^{PVHC} \ge 0 \tag{24}$$

where r_{ij} and x_{ij} represent the resistance and reactance of branch ij, respectively; $P_{s,t,ij}$ and $Q_{s,t,ij}$ represent the active power and reactive power flowing from bus i to bus j on branch at time t under scenario s, respectively; $U_{s,t,i}$ represents the voltage magnitude at bus i at time t under scenario s; $P_{s,t,i}$ and $Q_{s,t,i}$ represent the total active power and reactive power injected at bus i at time t under scenario s, respectively; $P_{s,t,i}^{DG}$ and $Q_{s,t,i}^{DG}$ represent the active power and reactive power injected by distributed generation (DG) at bus i at time t under scenario s, respectively; $P_{s,t,i}^{LOAD}$ and $Q_{s,t,i}^{LOAD}$ represent the active power and reactive power consumed by the load at bus i at time t under scenario s, respectively; $P_{s,t,i}^{EV}$ represents the active power of the electric vehicle (EV) charging station connected at bus i at time t under scenario s; P_i^{PVHC} represents the allowable active power increase that can be accommodated by PV integration at bus i.

5) Operational Constraints of the DN

To ensure the safe operation of the DN, practical operational limits are imposed on bus voltages and branch currents.

$$U_{\min}^2 \le U_{s,t,i}^2 \le U_{\max}^2 \tag{25}$$

$$0 \le I_{s,t,ij}^2 \le I_{\max}^2 \tag{26}$$

where $U_{\min}$ and $U_{\max}$ represent the maximum and minimum allowable voltage magnitudes for the DN buses, respectively; $I_{\max}$ represents the maximum allowable branch current value for the DN.

C. Linearisation Transformation And Solution Methods for the Proposed Model

To transform the model into a mixed-integer second-order cone programming (MISOCP) problem, new optimization variables are defined as the square of the bus voltage magnitude and the square of the branch current magnitude. By substituting these variables, the quadratic terms of bus voltages and branch currents in the objective function and constraints are eliminated.

$$u_{s,t,i} = U_{s,t,i}^2 \tag{27}$$

$$i_{s,t,i} = I_{s,t,i}^2 \tag{28}$$

The DN active power loss cost (4), power flow constraints (18)-(21) and operational constraints (27)-(28) are transformed into the following forms:

$$f^{loss} = \sum_{t=1}^{T} \sum_{ij\in\Omega_b} r_{ij} i_{s,t,ij} \tag{29}$$

$$\sum_{ji\in\Omega_b} \left(P_{s,t,ji} - r_{ij} i_{s,t,ij}\right) + P_{s,t,i} = \sum_{ik\in\Omega_b} P_{s,t,ik} \tag{30}$$

$$\sum_{ji\in\Omega_b} \left(Q_{s,t,ji} - x_{ij} i_{s,t,ij}\right) + Q_{s,t,i} = \sum_{ik\in\Omega_b} Q_{s,t,ik} \tag{31}$$

$$\begin{gathered} u_{s,t,i} - u_{s,t,j} + \left(r_{ij}^2 + x_{ij}^2\right) i_{s,t,ij} - \\ 2\left(r_{ij} P_{s,t,ij} + x_{ij} Q_{s,t,ij}\right) = 0 \end{gathered} \tag{32}$$

$$i_{s,t,ij} u_{s,t,i} = P_{s,t,ij}^2 + Q_{s,t,ij}^2 \tag{33}$$

$$U_{\min}^2 \le u_{s,t,i} \le U_{\max}^2 \tag{34}$$

$$0 \le i_{s,t,ij} \le I_{\max}^2 \tag{35}$$

However, the DN power flow constraint (33) remains a quadratic nonlinear constraint after variable substitution. Under the conditions that the objective function is a strictly increasing function of $i_{s,t,ij}$ and the bus load has no upper bound, it can be relaxed into a second-order cone constraint as follows:

$$\left\| \begin{matrix} 2P_{s,t,ij} \\ 2Q_{s,t,ij} \\ i_{s,t,ij} - u_{s,t,i} \end{matrix} \right\|_2 \le i_{s,t,ij} + u_{s,t,i} \tag{36}$$

The MISOCP model can be effectively solved by commercial mathematical programming solvers to determine optimal (DESS) planning schemes.

III. Case Study

A. Modified IEEE 33-bus Test Case

The modified IEEE 33-bus DN is selected to validate the effectiveness of the proposed DESS optimal planning model, as shown in Fig. 1. The DN is connected with 500 kW PV units at buses 5, 10, 13, 16, 22, and 25, and with 1000 kW and 1400 kW PV units at nodes 18 and 33, respectively. The total PV capacity of the DN is 5.4 MW. The load curve of the EV charging station is shown in Fig. 2. The base voltage of this test case is 12.66 kV, and the base capacity is 10 MVA.

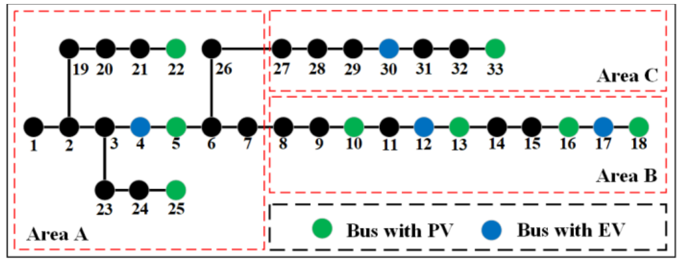

Fig. 1. Modified IEEE 33-bus distribution network.

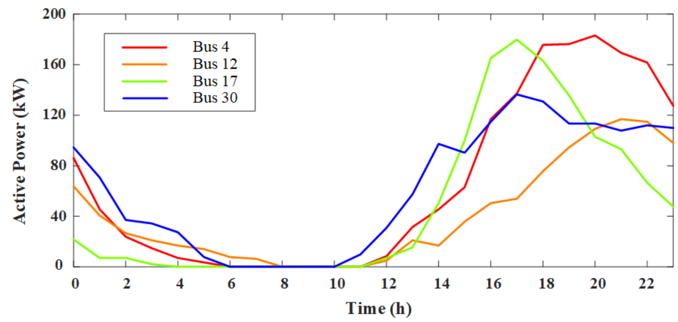

Fig. 2. The active power curve of the EV charging station.

To maximize the PVHC enhancement of the DN and ensure its safe operation, it is assumed that one DESS is configured in each area. The upper limit of the DESS capacity is set to 2 MWh. The unit planning capacity of DESS is 0.01 MWh and the unit planning power is 0.01 MW. The DESS basic parameters are listed in Table I.

TABLE I. DESS Parameters

Parameter	Value
Discount Rate	0.05
Service Life	15
Operation and Maintenance Coefficient	0.01
Unit Capacity Investment Cost(CNY/kVA)	350
Unit Power Investment Cost (CNY/kVA)	750
Maximum of SOC	0.8
Minimum of SOC	0.2
Charging Efficiency	0.9
Discharging Efficiency	0.9

In the typical operation scenario, the unit cost of the DN losses is 0.8 CNY/kWh. The PVHC enhancement benefit coefficient in the PVHC enhancement scenario is 2300 CNY/MW. The PV and load output curves with 24-hour intervals are shown in Fig. 3.

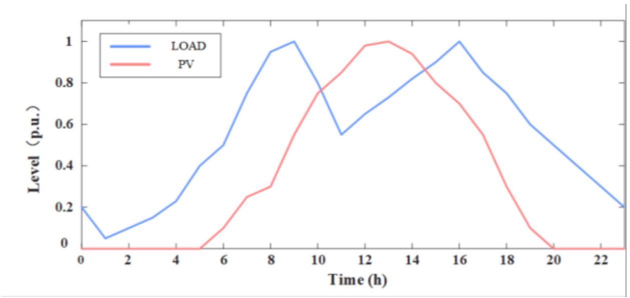

Fig. 3. PV and load output curves.

B. Effectiveness and Validation of DESS Planning Scheme

To fully validate the effectiveness of the proposed planning scheme and demonstrate the significant impact of DESS planning on the PVHC enhancement of the DN, the following three schemes are compared and analyzed for the aforementioned test case:

Scheme A: Obtain the initial operating state of the distribution network without DESS planning.

Scheme B: Consider only the economic operation of the DN with DESS planning.

Scheme C: Consider comprehensively both the economic operation of the DN and the PVHC enhancement benefits with DESS planning.

TABLE II. OPTIMIZATION RESULTS UNDER DIFFERENT SCHEMES

Cost	Scheme A	Scheme B	Scheme C
Total Cost (10,000 CNY)	/	124.95	124.31
DESS Construction & Maintenance Cost (10,000 CNY)	/	112.58	114.77
DN Loss Cost (10,000 CNY)	20.69	12.37	12.35
PVHC Benefit Cost (10,000 CNY)	/	/	-2.81
PVHC Enhancement (MW)	9.27	11.45	12.23
Bus Voltage Range (p.u.)	0.94-1.08	0.95-1.05	0.95-1.05

TABLE III. OPTIMAL DESS PLANNING FOR METHOD C

DN Area	DESS Installation Location	DESS Installation Capacity (kWh)	DESS Installation Power (kW)
Area A	5	370	140
Area B	18	1280	430
Area C	33	960	390

As shown in Table II, Scheme A presents the initial operating state of the DN, which exhibits issues such as voltage violations and high network losses. Scheme B optimizes the economic operation of the DN by configuring DESS, resulting in a reduction in DN loss costs compared to Scheme A, while also maintaining voltages within safe limits.

Compared to Scheme A and B, Scheme C improves the operating state of the DN by configuring DESS while fully considering the comprehensive costs of the DN. The operating state of the DESS configured at bus 18 in Scheme C is shown in Fig. 4. From the figure, it can be observed that the SOC of the DESS fluctuates within the normal allowable range, and the charging and discharging of the DESS reach a balance within one cycle (24 hours). Compared to Scheme A, Scheme C reduces the DN loss cost by 40.2%, increases the PVHC of the DN by 31.9%, and reduces voltage violations.

It is worth noting that the construction and maintenance costs of DESS in Scheme C are slightly higher than those in Scheme B. This is due to the impact of PVHC enhancement, which leads to a slight increase in the capacity and power of the DESS. However, from the perspective of total cost, Scheme C still has lower costs, making its planning effect more optimal.

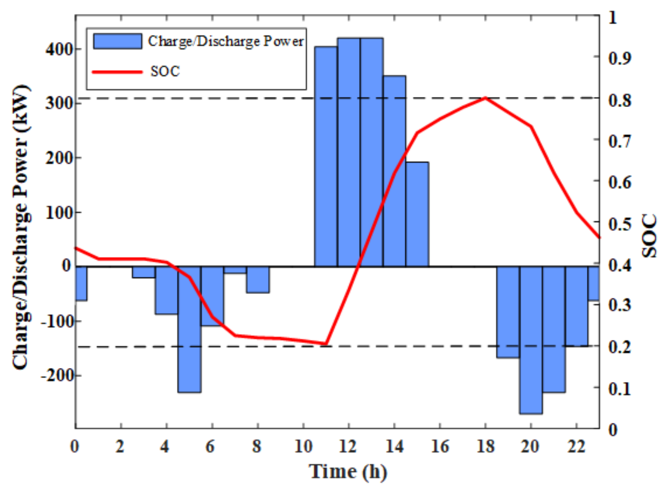

Fig. 4. DESS power and SOC change at bus 18 in Scheme C.

In Scheme A, the line losses are significant, and when the load demand peaks or PV output reaches its maximum, bus voltages exceed limits severely, resulting in poor economic operation of the DN. The voltage comparison at bus 18 between Scheme A and C is illustrated in Fig. 5.

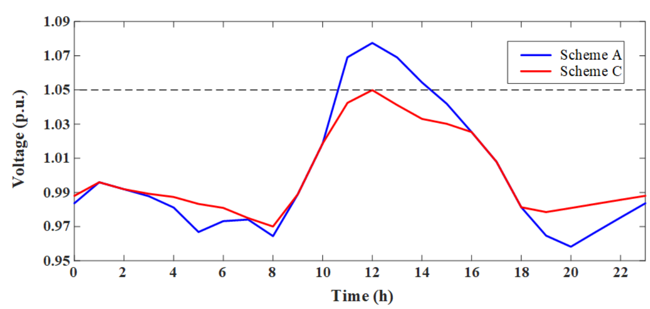

Fig. 5. Voltage comparison at bus 18 in Scheme A and C.

From Fig. 5, it can be observed that after the optimal planning of DESS in Scheme C, the voltage level of the DN is significantly improved. In Scheme A, the voltage rises to a maximum of 1.07 at 12:00 due to high PV generation, and drops to a minimum of 0.96 at 20:00 due to increased load demand. In contrast, in Scheme C, the maximum and minimum voltages at bus 18 are 1.05 and 0.97, respectively, and the voltage fluctuates within the allowable safe range [0.95, 1.05] throughout the day. This avoids voltage violations at the feeder end during heavy load conditions and voltage exceedance at PV connection points during high PV generation, ensuring the safety and reliability of the DN while also reducing line loss costs.

IV. CONCLUSION

To address the planning and operation requirements of future DNs with densely integrated PV, this paper proposes a DESS siting and sizing method considering PVHC enhancement. The proposed optimization model improves PVHC while reducing operational costs, enabling efficient renewable energy utilization and ensuring the secure operation of DNs.

However, this study has certain limitations, such as the assumption of uniform energy storage technologies in the planning model. The impact of different energy storage types (e.g., lithium-ion, flow batteries, or hybrid systems) on PVHC enhancement remains an open question and may influence cost, scalability, and performance. Future research should explore these technological variations, along with dynamic grid conditions and policy constraints. Additionally, real-world validation through case studies or pilot projects could further strengthen the practical applicability of the proposed method.

REFERENCES

[1] S. Bouguerra, M. R. Yaiche, O. Gassab, A. Sangwongwanich and F. Blaabjerg, "The impact of pv panel positioning and degradation on the PV inverter lifetime and reliability," *IEEE Journal of Emerging and Selected Topics in Power Electronics*, vol. 9, no. 3, pp. 3114-3126, June 2021.

[2] J. Zhao, Z. Zhang, H. Yu, H. Ji, P. Li and W. Xi, "Cloud-edge collaboration-based local voltage control for DGs with privacy preservation," IEEE Transactions on Industrial Informatics, vol. 19, no. 1, pp. 98-108, January 2023.

[3] Z. LUO, J. MA and Z. JIANG, "Research on power system dispatching operation under high proportion of wind power consumption," *Energies*, vol. 15, no.18, pp. 6819, March 2022.

[4] J. Jian, J. Zhao, H. Ji, L. Bai, J. Xu and P. Li, "Supply Restoration of Data Centers in Flexible Distribution Networks With Spatial-Temporal Regulation," in *IEEE Transactions on Smart Grid*, vol. 15, no. 1, pp. 340-354, January 2024.

[5] A. Koirala, T. Van Acker, R. Dhulst and D. Van Hertem, "Hosting capacity of photovoltaic systems in low voltage distribution systems: A benchmark of deterministic and stochastic approaches," *Renewable and Sustainable Energy Reviews*, vol. 155, pp. 115-122, May 2022.

[6] S. Wang, Y. Dong, L. Wu and B. Yan, "Interval overvoltage risk based pv hosting capacity evaluation considering PV and load uncertainties," *IEEE Transactions on Smart Grid*, vol. 11, no. 3, pp. 2709-2721, May 2020.

[7] M. Alturki, A. Khodaei and A.Paaso, "Optimization-based distribution grid hosting capacity calculations," *Applied Energy*, vol. 219, pp. 350-360, June 2018.

[8] S. Zhang, S. Ge, H. Liu, J. Li and C. Wang, "Model and observation of the feasible region for PV integration capacity considering Wasserstein-distance-based distributionally robust chance constraints," *Applied Energy*, vol 347, pp. 354-361, Apirl 2023.

[9] Y. Li, B. Feng, B. Wang and S. Sun, "Joint planning of distributed generations and energy storage in active distribution networks: A Bi-Level programming approach," *Energy*, vol 245, pp. 453-461, May 2022.

[10] N. Jayasekara, M. A. S. Masoum and P. J. Wolfs, "Optimal operation of distributed energy storage systems to improve distribution network load and generation hosting capability," *IEEE Transactions on Sustainable Energy*, vol. 7, no. 1, pp. 250-261, January 2016.

[11] M. J. E. Alam, K. M. Muttaqi and D. Sutanto, "Community energy storage for neutral voltage rise mitigation in four-wire multigrounded LV feeders with unbalanced solar PV allocation," *IEEE Transactions on Smart Grid*, vol. 6, no. 6, pp. 2845-2855, November 2015.